Proceedings of the Conference on Wavelet Analysis and Applications

Multiwavelets, Pseudodifferential Operators and Microlocal Analysis

Ryuichi ASHINO, Christopher HEIL, Michihiro NAGASE
and Rémi VAILLANCOURT

Dedicated to Professor Teruo Ikebe on the occasion of his seventieth birthday.

Abstract. Microlocal filtering is performed with adapted orthonormal multiwavelets, which are derived from several scaling functions. Microlocal filtering can also be considered to be the action of pseudodifferential operators whose symbols are characteristic functions of disjoint sets in Fourier space. Expansion of functions or signals in terms of an orthonormal multiwavelet basis gives a rough estimate of their microlocal content. A fast algorithm is presented and examples of filtered images are considered.
Keywords: multiwavelets, microlocal analysis, pseudodifferential operators.

1. Microlocal Analysis

Our approach to microlocal analysis for Schwartz distributions is based on the theory of hyperfunctions, as introduced by Sato [**1**] and exposed in [**2**] for the theory of linear partial differential equations with constant coefficients. A more complete treatment of microlocal filtering with multiwavelets can be found in [**3**].

Two important points are:

- Find directions along which a function can be continued analytically for every point $x \in \mathbb{R}^n$.
- A hyperfunction is defined as a sum of general boundary values of holomorphic functions in wedges whose edges are open subsets of $\mathbb{R}^n$.

2. One-Dimensional Hyperfunctions

Let $\delta(x)$ be the Dirac delta distribution. That is, $\delta(x)$ is the continuous linear functional which has the property that if the function $f(x)$ is continuous in a neighborhood of zero, then

$$\int_{\mathbb{R}} f(x)\delta(x)\,dx = f(0).$$

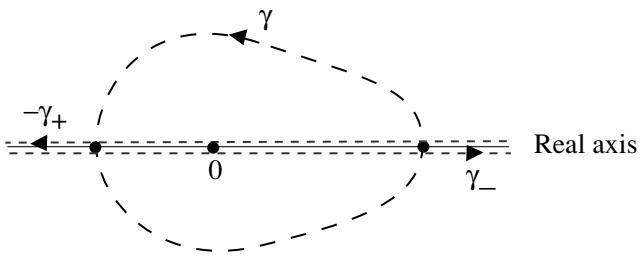

FIGURE 1. Shift of path γ to $-\gamma_+ + \gamma_-$.

On the other hand, if the function $f(z)$ is holomorphic in the closure of a domain $D \subset \mathbb{C}$, then by Cauchy's integral formula, we have

$$\frac{1}{2\pi i} \oint_\gamma \frac{f(z)}{z}\, dz = f(0), \qquad 0 \in D, \quad \partial D = \gamma.$$

Shifting the path γ to $-\gamma_+ + \gamma_-$, as shown in Fig. 1, gives the formula

$$\frac{1}{2\pi i} \oint_\gamma \frac{f(z)}{z}\, dz = \int_{-\infty}^{+\infty} \left(-\frac{1}{2\pi i}\right) \left(\frac{1}{x + i0} - \frac{1}{x - i0}\right) f(x)\, dx.$$

Thus, the Dirac delta measure admits the hyperfunction representation

$$\delta(x) = -\frac{1}{2\pi i} \left(\frac{1}{x + i0} - \frac{1}{x - i0}\right).$$

2.1. Definition of one-dimensional hyperfunctions.

- A hyperfunction $f(x)$, $x \in \mathbb{R}$, is defined as the difference of boundary values along $\mathbb{R}$ of two holomorphic functions:

  $$f(x) = F_+(x + i0) - F_-(x - i0),$$

  where $F_+(z)$ and $F_-(z)$ are holomorphic in $\{\mathrm{Im}\, z > 0\}$ and $\{\mathrm{Im}\, z < 0\}$, respectively.
- The defining functions $F_\pm(z)$ are not unique. Given any entire function $G(z)$, the same hyperfunction is defined by

  $$F_\pm(z) \qquad \text{and} \qquad F_\pm(z) + G(z).$$

2.2. Product of pairs of hyperfunctions. Assume

$$f(x) = F_+(x + i0), \qquad g(x) = G_+(x + i0),$$

where $F_+(z)$, $G_+(z)$ are holomorphic in $\{\mathrm{Im}\, z > 0\}$. In $\{\mathrm{Im}\, z > 0\}$, the product of $F_+(z)$ and $G_+(z)$ is

$$(F_+G_+)(z) := F_+(z)G_+(z).$$

- In taking the product of two hyperfunctions,

  $$f(x)g(x) := (F_+G_+)(x + i0),$$

  the directions of analyticity are important.

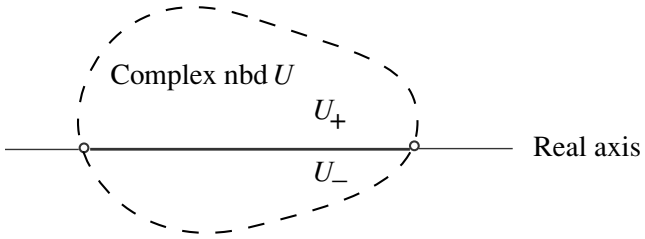

FIGURE 2. Complex neighborhoods U and $U_\pm$.

2.3. Microanalyticity. A close look at analyticity means a look at microanalyticity. Thus, for a complex neighborhood in the one-dimensional case, as shown in Fig. 2, we have the following definition of a microanalytic hyperfunction.

DEFINITION 1. *Let $\mathbb{S}^0 = \{\pm 1\}$. A hyperfunction $f(x)$ is said to be microanalytic at $(x; -1) \in \mathbb{R} \times \mathbb{S}^0$ if and only if there exists a complex neighborhood U of x such that both defining functions $F_\pm(z)$ of $f(x)$ can be extended analytically to the neighborhood $U_+ := U \cap \{\operatorname{Im} z > 0\}$.*

3. Microlocal Filtering

Given $f \in L^2(\mathbb{R}^n)$, let $f_{jk}(x)$ denote the scaled and shifted function

$$f_{jk}(x) = 2^{nj/2} f(2^j x - k), \qquad j \in \mathbb{Z}, \quad k \in \mathbb{Z}^n.$$

Let D be a finite index set. If $\{(\psi_\delta)_{jk}\}_{d\in D, j\in\mathbb{Z}, k\in\mathbb{Z}^n}$ is an orthonormal basis for $L^2(\mathbb{R}^n)$, then we say that $\Psi = [\psi_\delta]_{\delta\in D}$ is a multiwavelet function. The multiwavelet expansion of $f \in L^2(\mathbb{R}^n)$ with respect to this basis is

$$f = \sum_{\substack{\delta\in D \\ j\in\mathbb{Z}, k\in\mathbb{Z}^n}} \langle f, (\psi_\delta)_{jk} \rangle \, (\psi_\delta)_{jk}.$$

Problems.

- How can we construct two suitable multiwavelet functions $\psi_\pm$ corresponding to each microanalytic direction $\mathbb{S}^0 = \{\pm 1\}$?
- Is it possible to obtain information on the microlocal content of $f \in L^2(\mathbb{R})$ from the wavelet coefficients $(f, (\psi_\delta)_{jk})$?
- Can orthonormal multiwavelet filtering, which we call *microlocal filtering*, separate microlocal contents?

3.1. One-dimensional multiwavelets for microlocal filtering. To characterize the microanalyticity of a slowly increasing distribution $f \in \mathcal{S}'(\mathbb{R}^n)$ by its Fourier transform $\hat{f}$, we introduce the *dual cone*, Γ°, of Γ, defined by

$$\Gamma^\circ := \{\xi \in \mathbb{R}^n; y \cdot \xi \geq 0 \text{ for every } y \in \Gamma\}.$$

Examples of cones Γ, dual cones Γ° of cones Γ, and complements $(\Gamma^\circ)^c$ of dual cones Γ° are shown in Fig. 3.

LEMMA 1. *Let Γ be an open convex cone. A slowly increasing distribution $f(x) \in \mathcal{S}'(\mathbb{R}^n)$ can be represented as the limit $f(x + i\Gamma 0)$ of a slowly increasing holomorphic function $f(z)$ in the infinitesimal wedge $\mathbb{R}^n + i\Gamma 0$ if and only if the Fourier transform $\hat{f}$ of f is exponentially decreasing in the open cone $(\Gamma^\circ)^c$, the*

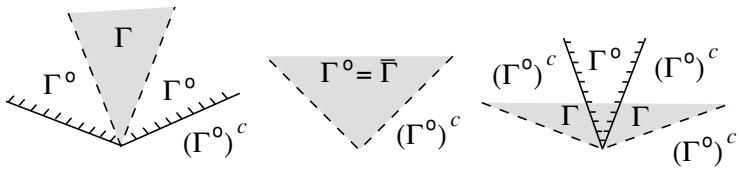

FIGURE 3. Open cone Γ, dual cone Γ°, and complement $(\Gamma^\circ)^c$ of dual cone.

FIGURE 4. The Fourier transform of $\psi_\pm$.

complement of the dual cone Γ°, that is, $\hat{f}$ is exponentially decreasing on every closed proper subcone $\Gamma' \subset\subset (\Gamma^\circ)^c$.

THEOREM 1. *Define $\psi_\pm$ by $\widehat{\psi}_\pm = \chi_{[\pm 2\pi, \pm 4\pi]}$ (see Fig. 4). Then $\Psi := {}^t(\psi_+, \psi_-)$ is a multiwavelet function. Define the orthogonal projections $\mathcal{P}_\pm$ by*

$$\mathcal{P}_\pm f := \sum_{j,k\in\mathbb{Z}} \langle f, (\psi_\pm)_{jk} \rangle \, (\psi_\pm)_{jk}.$$

Then $\mathcal{P}_\pm f(x)$ can be extended analytically to $\{\operatorname{Im} z > 0\}$ and $\{\operatorname{Im} z < 0\}$, respectively.

- This orthonormal basis is known [**4**].

Define the classical Hardy spaces $H^2(\mathbb{R}_\pm)$ by

$$H^2(\mathbb{R}_\pm) = \big\{ f \in L^2(\mathbb{R}) : \ \widehat{f}(\xi) = 0 \quad \text{a.a.} \ \ \xi \le (\ge) \, 0 \big\}.$$

Then

$$L^2(\mathbb{R}) = H^2(\mathbb{R}_+) \oplus H^2(\mathbb{R}_-).$$

Each $\psi_\pm$ is a uniwavelet function of $H^2(\mathbb{R}_\pm)$, respectively.

3.2. Definition of n-dimensional hyperfunctions. The following points are relevent to the n-dimensional case.

- In the n-dimensional case, the set of all microanalytic directions is the unit sphere $\mathbb{S}^{n-1}$, which is an infinite set.
- A generalization of Theorem 1 to the n-dimensional case is Theorem 2 below.
- It is possible to tell fairly well the directions along which f is microanalytic.
- The price to pay to get good angular resolution in $\mathbb{S}^{n-1}$ is the need for many multiwavelets.

DEFINITION 2. *A hyperfunction $f(x)$ in $\mathbb{R}^n$ is defined as a sum of the form*

$$f(x) = \sum_{j=1}^{N} F_j(x + i\Gamma_j 0), \qquad x \in \Omega,$$

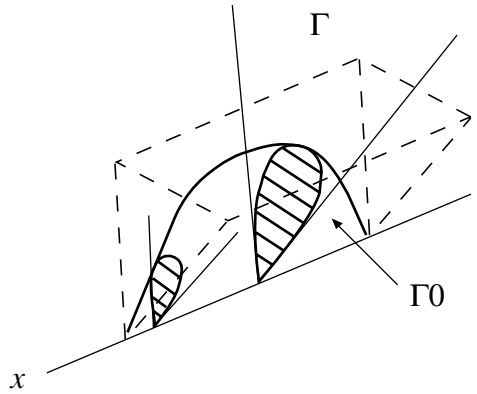

FIGURE 5. Infinitesimal wedge Γ0.

of boundary values

$$F_j(x + i\Gamma_j 0) = \lim_{\substack{y \to 0 \\ y \in \Gamma_j 0}} F_j(x + iy)$$

of holomorphic functions $F_j(z)$ *in infinitesimal wedges* $\Gamma_j 0$ *with edge* $\Omega \subset \mathbb{R}^n$ (see Fig. 5).

3.3. n-dimensional multiwavelets for microlocal filtering.

NOTATION 1. *We shall use the following notation in* $\mathbb{R}^n$.

- $\eta = (\eta_1, \ldots, \eta_n) \in H := \{\pm 1\}^n$, *parametrization of* 2^n *orthants in* $\mathbb{R}^n$.
- $\varepsilon = (\varepsilon_1, \ldots, \varepsilon_n) \in E := \{0, 1\}^n \setminus \{0\}$, $2^n - 1$ *vertices of unit cube, less the origin.*
- $\varepsilon . * \eta := (\varepsilon_1 \eta_1, \ldots, \varepsilon_n \eta_n)$.
- $Q_\eta := \prod_{k=1}^n [0, \eta_k]$, *unit cube, where* $[0, -1]$ *means* $[-1, 0]$.
- $\mathcal{Q}_{j,\varepsilon,\eta} := \left\{ \prod_{k=1}^n [\eta_k(\ell_k - 1), \eta_k \ell_k] + 2^j(\varepsilon . * \eta) : 1 \le \ell_1, \ldots, \ell_n \le 2^j, \ \ell_1, \ldots, \ell_n \in \mathbb{N}, \ j \in \mathbb{Z}_+ \right\}$.
- $\mathcal{Q} := \{Q_k\}_{k \in K}, \quad \iota(\mathcal{Q}) := \bigcup_{k \in K} Q_k$.
- $2\pi\mathcal{Q}_{j,\varepsilon,\eta} := \{2\pi Q \ ; \ Q \in \mathcal{Q}_{j,\varepsilon,\eta}\}$.
- $\mathbb{Z}_+^{E \times H}$ *is the set of all functions from* $E \times H$ *to* $\mathbb{Z}_+$.

THEOREM 2. *Let* $j \in \mathbb{Z}_+$, $\varepsilon \in E$, $\eta \in H$. *For* $Q \in \mathcal{Q}_{j,\varepsilon,\eta}$, *define* ψ_Q *by*

$$\widehat{\psi}_Q = \chi_{2\pi Q},$$

where $\chi_{2\pi Q}$ *is the characteristic function of the cube* $2\pi Q$. *For* $\rho \in \mathbb{Z}_+^{E \times H}$, *let*

$$\mathcal{Q}_\rho := \bigcup_{(\varepsilon,\eta) \in E \times H} 2\pi \mathcal{Q}_{\rho(\varepsilon,\eta),\varepsilon,\eta}.$$

Then $\Psi := (\psi_Q)_{Q \in \mathcal{Q}_\rho}$ *is a multiwavelet function.*

4. Two-Dimensional Masks

Figure 6 shows multiwavelets as masks or characteristic functions of cubes in Fourier space.

Figures 7 and 8 illustrate the prefiltering and filtering process of images in Fourier space.

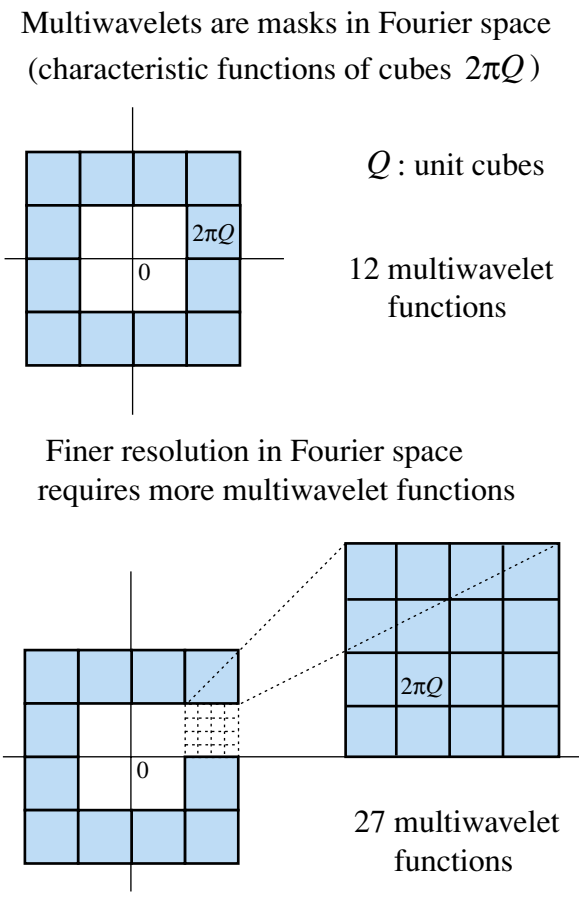

FIGURE 6. Multiwavelet masks and submasks.

5. Pseudodifferential Representation

Given an image $f(x, y)$ and a mask $p(\xi, \eta) = \chi_Q(\xi, \eta)$, filtering of f by p is represented by the pseudodifferential operator

$$\begin{aligned} Pf(x,y) &= \frac{1}{4\pi^2} \int_{\mathbb{R}^2} e^{i(x\xi+y\eta)} p(\xi,\eta) \hat{f}(\xi,\eta)\, d\xi\, d\eta \\ &= \frac{1}{4\pi^2} \int_{Q} e^{i(x\xi+y\eta)} \hat{f}(\xi,\eta)\, d\xi\, d\eta. \end{aligned}$$

Pseudodifferential operators, $P : f \mapsto Pf$ are pseudolocal operators, that is, they are not local operators but they do not spread or displace the singular support of f.

Micro-elliptic operators are studied in [**5**]. Nonlinear heat operators, which are hypoelliptic operators, are used to denoise images [**6**], [**7**].

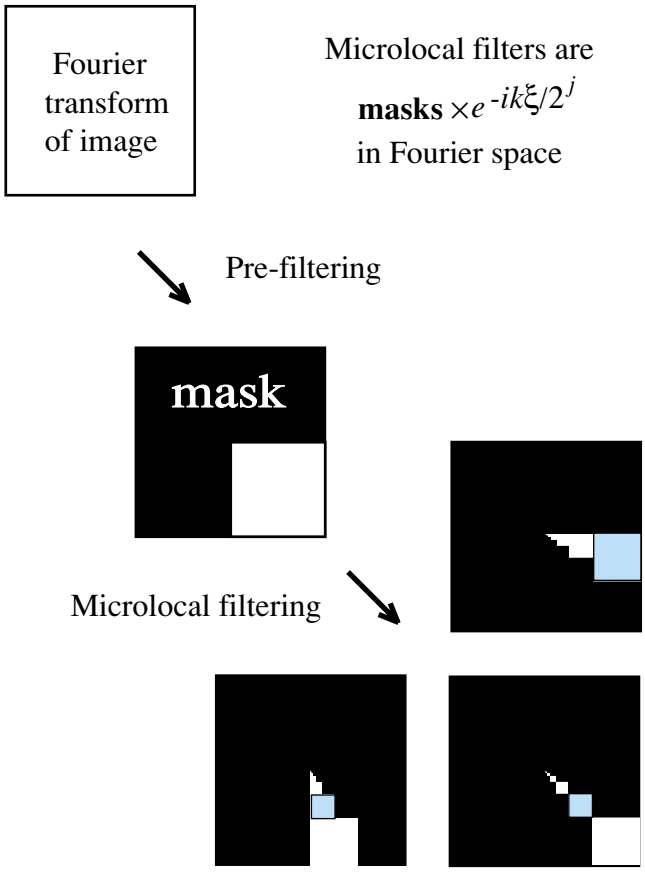

FIGURE 7. Multiwavelet masks of the fourth quadrant.

6. Separation of Singularities in an Image

The four figures in the left part of Fig. 9 are the prefiltered images of the "woman" image corresponding to the four prefilters with support in the four quadrants of the Fourier space, $(+,+)$, $(-,+)$, $(-,-)$, and $(+,-)$, taken counterclockwise, as shown in the top part of Fig. 8. The four figures in the right part of Fig. 9, taken in the counterclockwise direction starting with the top right image are (a) the original image and the result of its prefiltering by (b) $P_{(+,-)} + P_{(-,-)}$, (c) $P_{(+,-)} + P_{(-,+)}$, and (d) $P_{(+,-)} + P_{(+,+)}$.

The 12 filtered images of the "woman" image by means of the 12 multiwavelet masks of Fig. 8 and its Fourier transform are shown in Fig. 10. Fourier transforms of natural images often consist of a few high peaks corresponding to the smooth approximation of the image by the scaling functions and much smaller values corresponding to the details by the multiwavelets.

In this example, the prefiltered image by $P_{(+,-)}$ has maximum energy among the four prefiltered images by $P_{(\pm,\pm)}$, because it is the brightest. The following tableau lists the energy of the four prefiltered images.

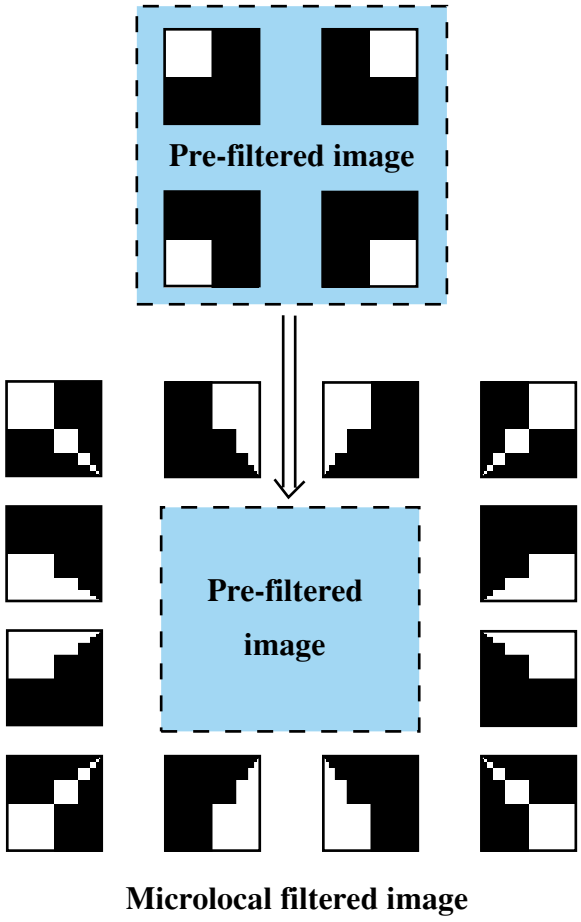

FIGURE 8. The twelve multiwavelet masks.

FIGURE 9. Left: the four prefiltered images. Right: top right, the original image, and three approximations (see text).

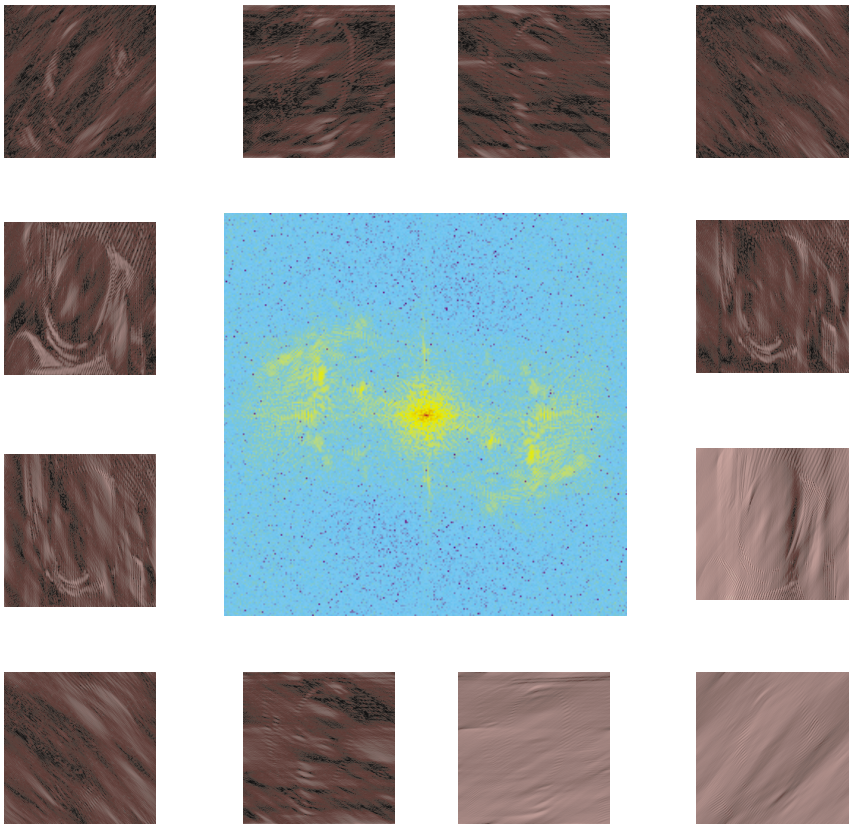

FIGURE 10. The Fourier transform (center) and the 12 microlocal filtered images (around) of the "woman" image.

```
Energy of 4 prefiltered images  =   1.0e+06 *
                      2.2059     2.0735
                      2.5749     8.5187
```

It is observed experimentally that the singular parts, or details, of an image contain less energy than its regular parts, or approximations. Hence it is conjectured that the prefiltered image by $P_{(+,-)}$ contains most of its regular parts and the other three prefiltered images contain most of its singular parts. This is observed in the prefiltered images by $P_{(+,-)} + P_{(-,-)}$, $P_{(+,-)} + P_{(-,+)}$, and $P_{(+,-)} + P_{(+,+)}$.

In the first case, the support of the Fourier transform of the prefiltered image by $P_{(+,-)} + P_{(-,-)}$ is contained in the lower half-space $\{(\xi, \eta) \in \mathbb{R}^2;\ \eta \leq 0\}$. Hence, Lemma 1 implies that there exists an open cone Γ_1 containing $(\xi, \eta) = (0, -1)$ and a holomorphic function $f_1(z)$ in the infinitesimal wedge $\mathbb{R}^2 + i\Gamma_1 0$ such that the filtered image by $P_{(+,-)} + P_{(-,-)}$ is represented as the limit $f_1(x + i\Gamma_1 0)$.

Similarly, in the third case, the support of the Fourier transform of the prefiltered image by $P_{(+,-)} + P_{(+,+)}$ is contained in the right half-space $\{(\xi, \eta) \in \mathbb{R}^2;\ \xi \geq 0\}$. Hence, by Lemma 1 there exists an open cone Γ_2 containing $(\xi, \eta) = (1, 0)$ and a holomorphic function $f_2(z)$ in the infinitesimal wedge $\mathbb{R}^2 + i\Gamma_2 0$ such that the filtered image by $P_{(+,-)} + P_{(+,+)}$ is represented as the limit $f_2(x + i\Gamma_1 0)$.

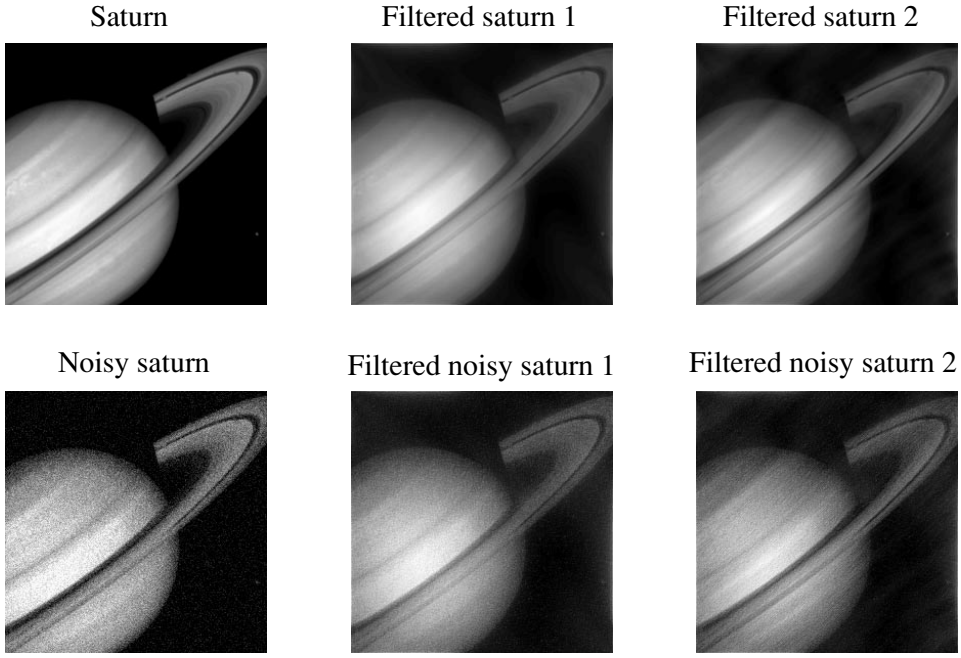

FIGURE 11. Nonnoisy (top) and noisy (bottom) "Saturn" images.

Hence these two filtered images by $P_{(+,-)} + P_{(-,-)}$ and $P_{(+,-)} + P_{(+,+)}$ are, in a sense, "approximations" of the original image.

In the second case, however, the support of the Fourier transform of the prefiltered image by $P_{(+,-)} + P_{(-,+)}$ cannot be contained in any half space. Hence, we may assume that the Fourier transform of the filtered image by $P_{(+,-)} + P_{(-,+)}$ cannot have exponential decay on any half-space (this is an assumption in dealing with images). Then the filtered image by $P_{(+,-)} + P_{(-,+)}$ cannot be represented as a boundary value of a single holomorphic function in an infinitesimal wedge but it can be represented as a sum of boundary values of several holomorphic functions in infinitesimal wedges. This means that the filtered image by $P_{(+,-)} + P_{(-,+)}$, in a sense, may be a "detail" only. These "regularities" and "singularities" can be seen in Fig. 9.

7. Microlocal Filtering of a Nonnoisy and Noisy Image

A Gaussian noise of zero mean and variance equal to 0.005 is added to the "Saturn" image. The original and noisy images are shown in the left part of Fig. 11.

The four prefiltered and the twelve microfiltered images of the noisy image are shown in Fig. 12. The energy in each of the twelve filtered parts, as measured by the Frobenius norm, is shown in the following tableau:

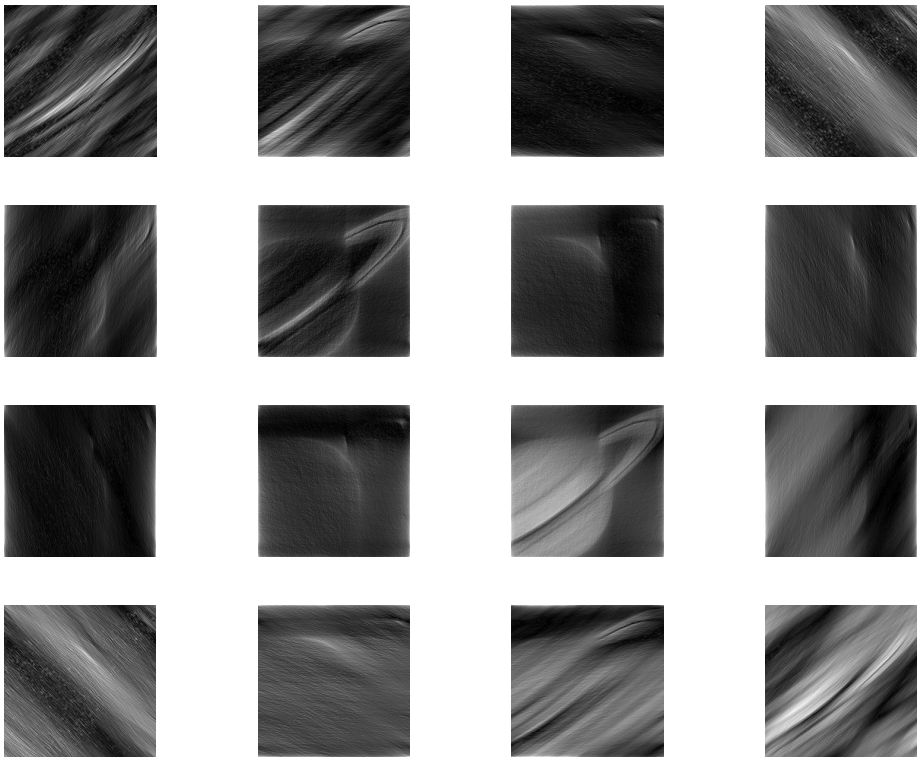

FIGURE 12. The four prefiltered (center) and the 12 microlocal filtered (around) images of the noisy "Saturn" image.

```
Energy = 1.0e+06 *

    0.8632    1.2849    0.8778    0.7957
    1.1707         0         0    1.3954
    1.1229         0         0    2.9633
    0.8322    1.4608    2.6909    2.4393
```

It is seen that the energy in the lower right corner is larger than in the remaining entries.

The filtered Saturn and noisy Saturn images 1 are reconstituted from the sum of the five lower right parts of Fig. 12 and are shown in the central part of Fig. 11.

The filtered Saturn and noisy Saturn images 2, shown in the right part of Fig. 11 are more completely reconstituted by adding the top left part of Fig. 12 to the above images 1.

The following tableau lists the noise level in each of the 12 filtered parts.

```
Energy =

    775.0441  784.5579  777.4827  787.3333
    776.8823         0         0  779.2572
    779.3348         0         0  990.3241
    786.4254  778.1941  997.4562  991.4474
```

Since the noise is somewhat evenly distributed, it is reduced by a factor of 5/12 in the reconstructed images 1 which use five out the twelve filtered parts and by a factor of 6/12 in the reconstructed images 2 which use six out the twelve filtered parts. In both reconstructions, the Saturn ring along the secondary diagonal is rendered to a satisfactory degree.

References

[1] M. Sato, *Theory of hyperfunctions I* J. Fac. Sci. Univ. Tokyo, Sec. I, **8**(1) (1959) 139–193.
[2] A. Kaneko, *Linear partial differential equations with constant coefficients*, Iwanami, Tokyo, 1992. (Japanese)
[3] R. Ashino, C. Heil, M. Nagase, and R. Vaillancourt, *Microlocal filtering with multiwavelets*, Computers & Mathematics with Applications, **41** (2001), to appear.
[4] I. Daubechies, A. Grossmann, and Y. Meyer, *Painless nonorthogonal expansions*, J. Math. Phys., **27**(5) (1986) 1271–1283.
[5] L. Hörmander, *The analysis of linear partial differential operators III*, Springer-Verlag, Berlin, 1985, Chapter 22.
[6] S. Mallat, *A wavelet tool of signal processing*, Academic Press, San Diego, 1998, Sections 5.5 and 6.3.
[7] L. Alvarez, P.-L. Lions, and J.-M. Morel, *Image selective smoothing and edge detection by nonlinear diffusion. II*, SIAM J. Numer. Anal., **26**(3) (1992) 845–866.

Division of Mathematical Sciences, Osaka Kyoiku University, Kashiwara, Osaka 582-8582, Japan
E-mail address: ashino@cc.osaka-kyoiku.ac.jp

School of Mathematics, Georgia Institute of Technology, Atlanta, Georgia 30332 USA
E-mail address: heil@math72.math.gatech.edu

Department of Mathematics, Graduate School of Science, Osaka University, Toyonaka, Osaka 560-0043, Japan
E-mail address: nagase@math.wani.osaka-u.ac.jp

Department of Mathematics and Statistics, University of Ottawa, Ottawa, Ontario, Canada K1N 6N5
E-mail address: remi@uottawa.ca